Eur. Phys. J. B (2016) 89: 233
DOI: 10.1140/epjb/e2016-70489-3

THE EUROPEAN PHYSICAL JOURNAL B

Regular Article

From solitons to discrete breathers

Manuel G. Velarde[1,a], Alexander P. Chetverikov[2], Werner Ebeling[3], Sergey V. Dmitriev[4,5], and Victor D. Lakhno[6]

[1] Instituto Pluridisciplinar, UCM, Paseo Juan XXIII 1, 28040 Madrid, Spain
[2] Department of Physics, Saratov State University, Astrakhanskaya 83, 410012 Saratov, Russia
[3] Institute of Physics, Humboldt University, Newton strasse 15, 12489 Berlin, Germany
[4] Institute for Metals Superplasticity Problems, Russian Academy of Sciences, Khalturin 39, 450001 Ufa, Russia
[5] Research Laboratory for Mechanics of New Nanomaterials, Peter the Great St. Petersburg Polytechnical University, 195251 St. Petersburg, Russia
[6] Institute of Mathematical Problems of Biology, Russian Academy of Sciences, Vitkevicha 1, 142290 Pushchino, Russia

Received 19 August 2016 / Received in final form 30 August 2016
Published online 24 October 2016 –

Abstract. The excitation of solitons and discrete breathers (pinned or otherwise, also known as intrinsic localized modes, DB/ILM) in a one-dimensional lattice, also denoted as a chain, is considered when both on-site and inter-site vibrations, coupled together, are governed by the empirical Morse interaction. We focus attention on the transformation of the former into the latter as the relative strength of the on-site potential to that of the inter-site potential is increased.

1 Introduction

It was a surprising finding that spontaneously localized excitations, pinned or otherwise, may appear in a perfect crystal lattice [1–10]. They were denoted as discrete breathers, a.k.a. intrinsic localized modes (DB/ILM in what follows) and considered as genuinely due to the discrete character of the lattice which provides dispersion. The latter balanced by nonlinearity provides the support for the survival of such localized excitations. Breathers, nonlinear localized modes with internal time periodic structure, had earlier being described as solutions of the sine-Gordon and the nonlinear Schrödinger equations [11]. Other nonlinear localized excitations denoted as solitons are also known for perfect (anharmonic) lattices, like the Toda lattice, and continuum equations like the Boussinesq-Korteweg-de Vries equation whose soliton solutions are also long wave excitations in the discrete approximation for the numerical exploration of the equations in the continuum [11–15]. In the latter there is also an appropriate balance between dispersion (velocity depends on color/wavelength) and nonlinearity (velocity depends on amplitude) leading to the survival of the corresponding solitons. That localization of excitations is possible in crystals is to be expected when defects or disorder occur along the lattice structure (Anderson localization and the like [16,17]).

In general, there are on-site and inter-site interactions in a crystal lattice (have in mind the corresponding Einstein and Debye primitive models of a solid). Most of the mathematical proofs of existence of DB/ILM start in the anti-continuum limit which is a caricature of a crystal lattice when the on-site dynamics largely overwhelms the inter-site dynamics [9,18–20]. If one thinks of units with strong on-site dynamics coupled to the others, say the two nearest-neighbors, by weak inter-site potentials one may guess that one among them could at a certain moment benefit from the others thus attaining a spontaneous growth that eventually could persist, with corresponding slaving of the others who may also benefit, if circumstances are appropriate. This is a typical case of opportunism, cooperative or otherwise (for an in-depth and extensive study of this concept and related matters see Ref. [21]).

Here we shall concentrate on a one-dimensional model where both on-site and inter-site vibrations are governed by empirical Morse interactions. Our aim is to uncover possibilities offered by varying their relative significance. We shall show that both solitons and DB/ILM (pinned or otherwise) are possible. Furthermore, we shall show how one mode appears and eventually transforms into the other as we vary appropriate parameters (a unified mathematical description of solitons and breathers is provided in Ref. [20]). We have in mind that discreteness provides bounds and gaps to the spectrum of linear oscillations whereas nonlinearity makes the amplitude of oscillations frequency-dependent. We also have in mind that the inter-site Morse potential favors the excitation of soliton-like modes. It also permits the onset of (pinned) DBs albeit with some constraints, like being assisted by on-site oscillations, due to its "soft" character (frequency of small

[a] e-mail: mgvelarde@pluri.ucm.es

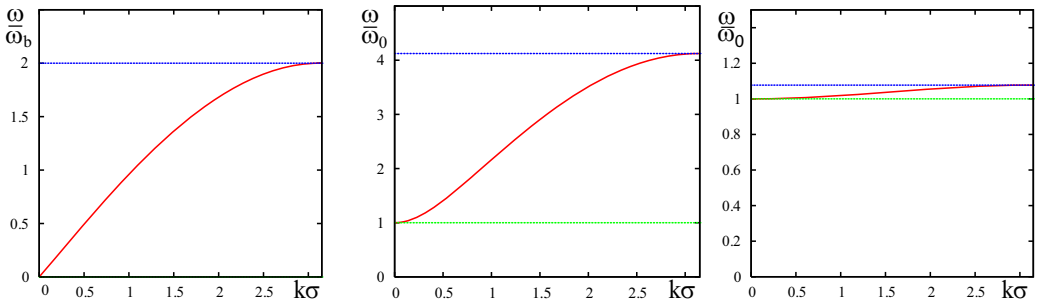

Fig. 1. Brillouin dispersion relation (half) plots (with appropriate dimensionless units) for a lattice of identical oscillators. Extreme left panel: chain of point particles, $\omega_0 = 0$ (no on-site potential; gapless); central panel: general case, $\omega_0 \sim \omega_b$ (here, in particular, $\omega_b = 2\omega_0$; non-zero gap); and extreme right panel: very weak inter-site bond, $\omega_b \ll \omega_0$ (here $\omega_b = 0.2\omega_0$; non-zero gap). In each case the region between the solid (dispersion, red) line and the upper dotted (blue) line is the so-called "phonon" band whose size drastically depends on the strength of the on-site potential as we can see by going from the left to the right panels. The extreme right panel shows quite a narrow phonon band indeed.

amplitude oscillations around minimum decreases when amplitude increases; its well width goes outside the harmonic potential or, to put it differently, its spring stiffness decreases with the widening of the inter-site separation). DB/ILM could be mobile (subsonic or otherwise), pinned, or even impossible depending indeed on parameter values, whereas solitons would generally be supersonically moving [7–10]. Coupling the inter-site Morse potential to the on-site Morse potential offers a variety of possibilities as the latter favors the onset of DB (for the case of on-site harmonic oscillations coupled to inter-site harmonic oscillations see [22]). Note that DB/ILM are always possible with a 'hard' potential (frequency of small amplitude oscillations around the minimum increases with increasing amplitude or spring stiffness increases with the widening of the separation; otherwise in soft/hard the force is smaller/greater than the linear force alone). Note also that when two coupled harmonic oscillators are resonant, any amount of energy initially given to one of them alternates periodically between them with a frequency proportional to the strength of their coupling. Then in a lattice/chain with coupled identical harmonic oscillators there is energy propagation. In order for the energy to remain localized, resonance has to be broken and this is feasible when there are defects or disorder along the lattice. If, however, the oscillators are nonlinear as their frequencies depend on amplitude when two are coupled and energy is given to one of them in a way that its frequency is equal to the harmonic approximation of the other, resonance is generally broken after some energy transfer because the frequencies change and then the transfer stops. However, it was shown that resonance between two weakly coupled anharmonic oscillators may persist under particular conditions [18,19].

In Section 2 we pose the mathematical problem in the form of nonlinear evolution equations. Their solutions are discussed in Section 3 for two extreme opposite limiting cases of parameter values. Section 4 deals with the same problem in further generality. In Section 5 we sketch the role of transverse motions to the original one-dimensional lattice geometry. Finally Section 6 is devoted to a summary of results.

2 Lattice dynamics, dispersion relations and evolution equations

Before addressing the dynamics with Morse potentials it seems worth recalling results from the linear case. The evolution of small amplitude vibrations is generally described by a system of linear differential equations

$$\frac{d^2 r_n}{dt^2} = -\omega_0^2 r_n + \omega_b^2 \left(r_{n+1} - 2r_n + r_{n-1}\right), \qquad (1)$$

where r_n denotes the deviation from the equilibrium state of the element/unit/particle "n" and ω_0 and ω_b correspond, respectively, to the on-site and inter-site oscillations. Equation (1) accounts for both types of oscillations due to the symmetry of the parabolic potentials. Solutions are linear combinations of normal modes $r_n \sim \exp(i(\omega t - kn\sigma))$ with frequency ω and wave number k whose dispersion relation yields explicitly:

$$\omega^2 = \omega_0^2 + 4\omega_b^2 \sin^2\left(k\sigma/2\right), \qquad (2)$$

where σ is the equilibtrium inter-site distance. Figure 1 illustrates the correpponding (half) Brillouin plots. In general, there are two critical frequencies in a dispersive diagram of a chain of interacting oscillators: $\omega_{cr1} = \omega_0$ and $\omega_{cr2} = \sqrt{\omega_0^2 + 4\omega_b^2}$. The region $\omega_{cr1} < \omega < \omega_{cr2}$, with $\mathrm{Im}k(\omega) = 0$, and $\mathrm{Re}k(\omega) \neq 0$, is the "phonon" band in quantum language. Solutions corresponding to this band are travelling waves with constant amplitude. For $\omega < \omega_{cr1}$ and $\omega > \omega_{cr2}$ we have $\mathrm{Im}k(\omega) \neq 0$, $\mathrm{Re}k(\omega) = 0$ and we are outside, below or above, the phonon band, respectively.

Looking at Figure 1, we can guess that, provided adequate nonlinearity is added to the dynamics, lattice solitons are expected inside the phonon band when there is moderate wave dispersion (from around the center to the upper right corner of the dispersion line). DB/ILM can be searched for frequencies above ω_{cr2} and below ω_{cr1} (as long as the harmonics do not enter the phonon band). Inside the phonon band they are not possible since any resonance or harmonics with the extended phonons will

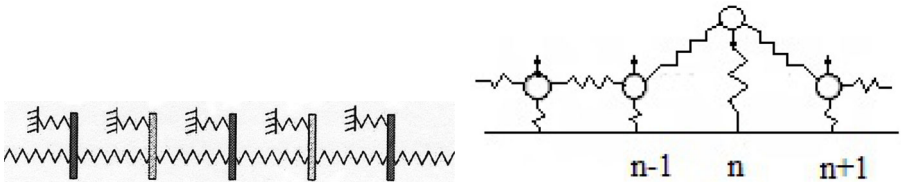

(a) (b)

Fig. 2. One-dimentional lattice of oscillators with (a) longitudinal and (b) transverse motions of units.

radiate the DB/ILM away. In view of the above after introducing the Morse potentials for both inter-site and on-site dynamics we have the following nonlinear evolution equations for identical particles of mass m

$$m\frac{d^2r_n}{dt^2}+\left[\left(\frac{\partial U_M^{\text{inter-site}}}{\partial r}\right)\Big|_{r=|r_{n+1}-r_n|}-\left(\frac{\partial U_M^{\text{inter-site}}}{\partial r}\right)\Big|_{r=|r_n-r_{n-1}|}\right]+\frac{\partial}{\partial r}U_M^{\text{on-site}}|_{r=r_n}=0 \tag{3}$$

with

$$r_n=x_n-x_{n0}=x_n-n\sigma$$

and

$$U_M=D\left(e^{-2br}-2e^{-br}\right),$$

where D and b characterize, respectively, the potential well depth (or dissociation energy level) and its stiffness; indexes "inter-site" and "on-site" refer to inter-site and on-site potentials, respectively. To simplify, thus limiting our study to a first approximation to the problem, we take $\sigma^{\text{on-site}}=\sigma^{\text{inter-site}}$. For universality in the argument and convenience in our discussion of cooperation and/or competition between the on-site and inter-site Morse potentials we rescale the problem using the following relationships: $\tau=\omega_M^{\text{inter-site}}t$, $\eta_b=b^{\text{on-site}}/b^{\text{inter-site}}$ (ratio of widths of potential wells/stiffnesses), and $\eta_D=D^{\text{on-site}}/D^{\text{inter-site}}$ (ratio of depths of potential wells). Also, a natural unity of velocity $v^{\text{inter-site}}=(\sigma\omega_M)^{\text{inter-site}}$ appears which corresponds to the sound velocity v_{sound} in a lattice without on-site potential (Fig. 1, left panel). This choice of units reflects our intention of illustrating the passage from (supersonic) moving solitons to DB/ILM, pinned or otherwise, along the same lattice as we vary the above defined ratios. In no case this represents a significant limitation of the study.

Thus in dimensionless variables the evolution equation (3) become

$$\frac{d^2q_n}{dt^2}=\left[1-e^{(q_n-q_{n+1})}\right]e^{(q_n-q_{n+1})}-\left[1-e^{(q_{n-1}-q_n)}\right]e^{(q_{n-1}-q_n)}-\eta_b\eta_D\left[1-e^{-\eta_b q_n}\right]e^{-\eta_b q_n} \tag{4}$$

with $q_n=b^{\text{inter-site}}r_n$ and $t\to t\omega_M$, where ω_M accounts for the small amplitude oscillations in the inter-site Morse potential well ($\omega_M^2=2(Db^2)^{\text{inter-site}}/m$).

Note that equations (3) and (4) refer to the case of a chain with longitudinal motion of particles only, as the opposite directions of propagation of wave excitations in such chain are not equivalent due to the asymmetry imposed by the Morse potential (Fig. 2a) in contrast to a chain with transverse motion of units (Fig. 2b) as e.g. in the Peyrard-Bishop (PB) model for DNA [11,23,24]. In such a case though the "longitudinal" distance between units (projections of deviations onto the original one-dimensional equilibrium lattice geometry) does not change, there are transverse deviations of the units (Fig. 2b) $y_{n0}=0$ and hence $r_n=y_n-y_{n0}=y_n$. Then the interaction of nearest neighbors depends on the relative difference of such transverse deviations.

Because both elements, $(n-1)$th and $(n+1)$th, impart motion on their nearest neighbor nth element equations (3) and (4) are equivalently written as follows:

$$m\frac{d^2r_n}{dt^2}+\left[\left(\frac{\partial U_M^{\text{inter-site}}}{\partial r}\right)|_{r=|r_n-r_{n+1}|}+\left(\frac{\partial U_M^{\text{inter-site}}}{\partial r}\right)|_{r=|r_n-r_{n-1}|}\right]+\frac{\partial}{\partial r}U_M^{\text{on-site}}|_{r=r_n}=0, \tag{3a}$$

$$\frac{d^2q_n}{dt^2}=-\left[1-e^{(q_{n+1}-q_n)}\right]e^{(q_{n+1}-q_n)}-\left[1-e^{(q_{n-1}-q_n)}\right]e^{(q_{n-1}-q_n)}-\eta_b\eta_D\left[1-e^{-\eta_b q_n}\right]e^{-\eta_b q_n}. \tag{4a}$$

3 Solitons and DB/ILM as extreme opposite limiting cases

Let us first consider the dynamics of the chain with solely longitudinal motion of particles ("longitudinal" lattice). In general equations (4) are not solved analytically and numerical simulation should be performed to have answers about the evolution of the lattice. However there are two extreme opposite limiting cases when it is possible to have approximate analytical descriptions of the evolution of nonlinear localized excitations: the soliton in a Morse

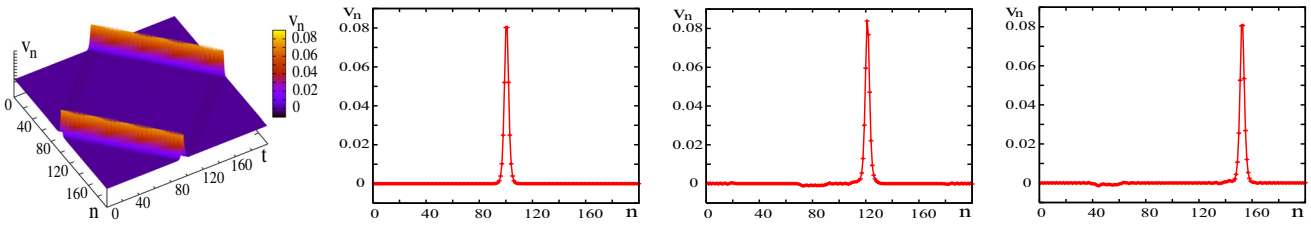

Fig. 3. Morse lattice, with periodic boundary conditions, without on-site potential ($N = 200$, $\kappa = 0.5$, $t = 0$–200). A low energetic lattice soliton (kinetic energy of particles are lower than D), embracing ten lattice units is introduced as initial condition (5). Left to right: evolution of velocity distribution $v_n(t)$ for the time interval $t = 0$–200, with snapshots at $t = 10$, 20 and 50. The soliton velocity is $v_{\rm sol} = 1.05$ in units of $v^{\text{inter-site}} = (\sigma\omega_M)^{\text{inter-site}}$ which is the sound velocity $v_{\rm sound}$ here (that is the linear velocity of the dynamics in the harmonic approximation to the Morse potential). Recall that in a soliton the velocity depends on amplitude/energy.

chain without on-site potential ($\eta_D = 0$) and the low-frequency pinned DB/ILM. In all computations presented in this work we use periodic boundary conditions.

Case 1: soliton in a Morse chain without on-site potential ($\eta_D = 0$)

With the Morse potential, at not very high energy (value relative to D) the lattice excitations are approximated within ten percent by the exact analytically known Toda solitons [14,25–27]. Thus, we set as an initial condition at $t = 0$

$$q_n = q_{n+1} + \frac{1}{3}\ln\left(1 + \frac{sh^2\kappa}{ch^2\left(\kappa\left(n - n_{\rm centr}\right) - sh\,\kappa t\right)}\right)$$

with

$$v_n = \frac{dq_n}{dt}, \tag{5}$$

where κ is the inverse width at half level of the excitation and $n_{\rm centr}$ is the location of its maximum height. Figure 3 illustrates its time and space evolution using equation (4).

Case 2: low-frequency pinned DB/ILM

In the simplest case when the on-site interaction largely overwhelms the inter-site force it may be assumed that a highly-energetic oscillation with a frequency appreciably lower than the low critical frequency (i.e., in the gap below the phonon band) is localized at a single site, for illustration here $n = n_0$. It is quite well captured by the solution of the Morse oscillator equation

$$\frac{d^2q_{n_0}}{dt^2} = -\eta_b\eta_D\left[1 - e^{-\eta_b q_{n_0}}\right]e^{-\eta_b q_{n_0}}, \tag{6}$$

which follows from equation (4) for large enough values of η_b and η_D thus leading to

$$\frac{d^2Q}{d\tilde{\tau}^2} = e^{-2Q} - e^{-Q} \tag{7}$$

with $Q = \eta_b q_{n_0}$ and $\tilde{\tau} = \eta_b\sqrt{\eta_D}t$. The exact analytical solution of (7) for initial conditions $Q = 0$ and $\tilde{v} = dQ/d\tilde{\tau} = \tilde{v}_0 < 1$ at $\tilde{\tau} = 0$ is:

$$Q = \ln\left[\frac{1 + \tilde{v}_0\sin\left(\sqrt{1-\tilde{v}_0^2}\tilde{\tau} - \arcsin\tilde{v}_0\right)}{1 - \tilde{v}_0^2}\right], \tag{8}$$

$$\tilde{v} = \frac{\tilde{v}_0\sqrt{1-\tilde{v}_0^2}\cos\left(\sqrt{1-\tilde{v}_0^2}\tilde{\tau} - \arcsin\tilde{v}_0\right)}{1 + \tilde{v}_0\sin\left(\sqrt{1-\tilde{v}_0^2} - \arcsin\tilde{v}_0\right)}. \tag{9}$$

Figure 4 graphically displays the result found which corresponds to the anti-continuum limit as the excitation of the Morse oscillators is akin to a weak coupling between them. One can observe a deviation from harmonic oscillations of the velocity of particles with (dimensionless) frequency $\tilde{\omega} = \sqrt{1-\tilde{v}_0^2}$ localized in a narrow region of the lattice. Then it appears that the expressions (8) and (9) describe quite accurately the behavior of the central site of a pinned breather for $n_0 = 50$, $v_0 < 1$ using equation (4). The DB/ILM embraces a few sites as illustrated in Figure 5.

Our aim now is to visualize the transformation of soliton-like waves (Fig. 3) to DB/ILM breather-like excitations (Fig. 5) when varying the values of the parameters η_b and η_D.

4 Solitons and DB/ILM as variations on a theme

Generally, solitons and DB/ILM are excited when using appropriate initial conditions alien one to the other. However to study different kinds of excitations including intermediate cases between solitons and pinned DB/ILM in a wide range of parameter values it seems reasonable to perturb the lattice using a kind of common initial condition though we are aware indeed of their different structure. The excitation of narrow highly-energetic structures, both soliton-like and breather-like, is made possible by using an initial perturbation in the form of a strong enough kick to a single unit ($v_n = q_n = 0$ for all n except one particle for which $v_{n0} = v_0 \neq 0$). Computer simulations show that localized waves accompanied by low energetic phonons are excited in a wide range of parameter values.

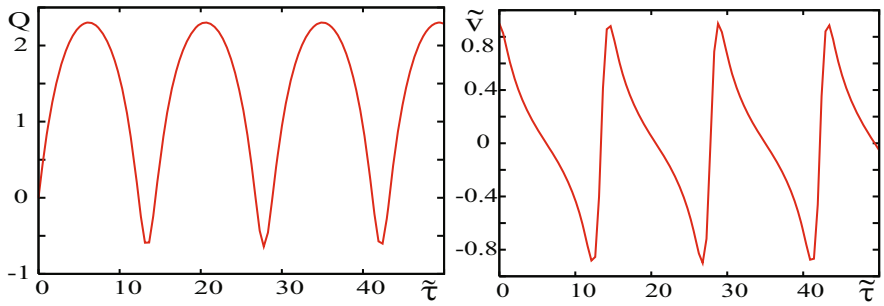

Fig. 4. Anharmonic oscillations of a Morse-oscillator: Q (left) and $\tilde{v}$ (right) vs. $\tilde{\tau}$ with $\tilde{v}_0 = 0.9$.

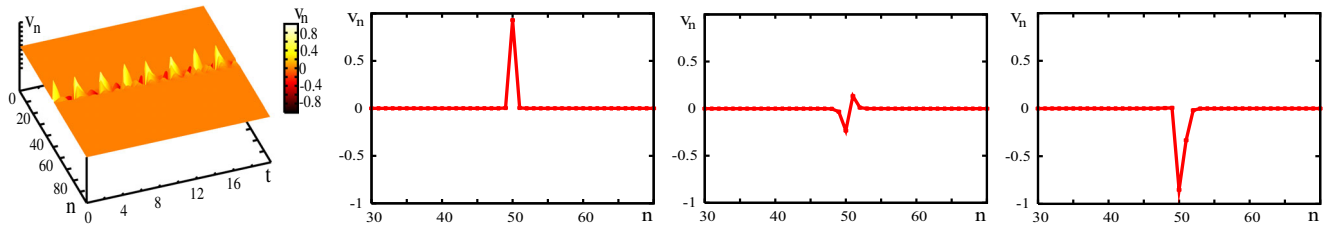

Fig. 5. Morse chain ($N = 100$). Low-frequency pinned DB/ILM when the on-site interaction largely overwhelms the inter-site force (time interval $t = 0$–20). Left to right: time evolution of the velocity distribution $v_n(t)$ (in units of $v^{\text{inter-site}}$ here) for $t = 20$, then snapshots at $t = 0.1$, 1.2 and 2. Recall that for a pinned DB/ILM the frequency depends on energy.

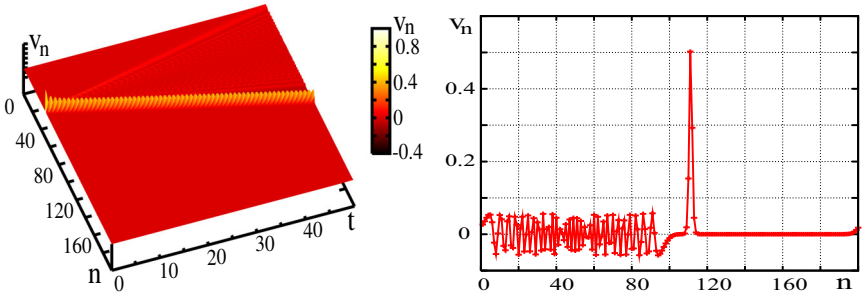

Fig. 6. Morse lattice ($N = 200$) without on-site potential ($\eta_b = \eta_D = 0$). Highly-energetic soliton (kinetic energy of particles is D or greater) excited by an initial kick to a unit, here $n = 50$ with $v_0 = 1$. The soliton velocity is 1.3 in units of the sound velocity (as it follows from simulation data: starting at site 70 the excitation reaches site 135 at time 50). Left panel: evolution of particles velocity distribution for time interval $t = 0$–50; right panel: particles velocity distribution at $t = 50$ (for comparison with Fig. 3, extreme left panel; there is a difference – the phonon "tail" in Fig. 6 due to larger difference in initial conditions from the real form of the soliton relative to Fig. 3 where the initial conditions fit better the real form of the soliton solution; note that the tail, as it is linear, hence sonic, lags *behind* the supersonic solitonic peak).

Figure 6 depicts a supersonic soliton formed very quickly from an initial delta function-like space distribution by kicking a single particle (on-site potential off). Figure 6 differs from Figure 3 by the different phonon background lagging behind the solitonic peak. But phonons do not significantly affect the evolution of highly-energetic localized nonlinear waves of different kinds and they may be neglected when analyzing the evolution of those waves. Besides, this phonon background may be erased in order to use the cleaned residual excitation as a new initial condition for continuing new computer simulations leading to the ultimate result illustrated in Figure 7. Clearly the latter differs from Figure 3 (extreme left panel) in much less degree than Figure 6. Such "erasing" procedure may be repeated to optimize computation time and the refinement of the ultimate form of the localized excitation.

To visualize the transformation of localized excitations in the parametric plane $\eta_b - \eta_D$ we performed a series of computer simulations for different values of η_b and η_D. The results are displayed in Figures 8 and 9 for constant $\eta_D = 0.4$ and varying η_d in the range between 0.5 and 8 (Fig. 8) and constant $\eta_b = 2$ and varying η_D in the range between 0.1 and 2 (Fig. 9). We should note that the asymmetry of the Morse potential to compressions-expansions (Fig. 2a) leads to the asymmetry in the moving solitons left-to-right and right-to-left. With a potential having symmetry the two directions of motion are identical. Here we consider the case when the excitation of mobile DB/ILM is with initial velocity $v_0 > 0$ and disregard the other possibility ($v_0 < 0$).

As it follows from Figures 8 and 9 a typical intermediate localized excitation looks (except Fig. 8c)

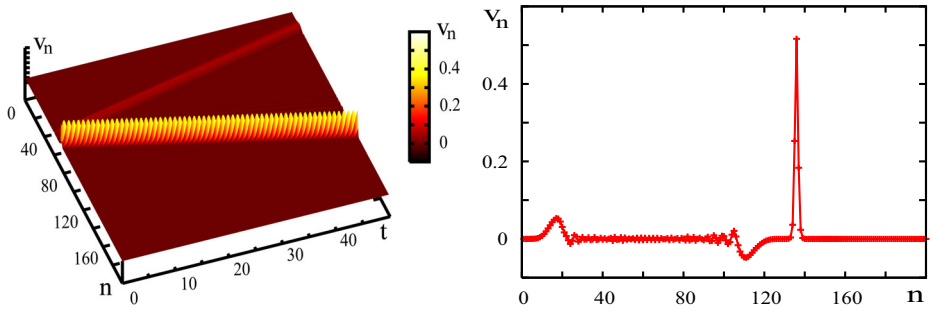

Fig. 7. Morse lattice ($N = 200$) without on-site potential ($\eta_b = \eta_D = 0$). Utimate soliton structure of the highly-energetic soliton of Figure 6 when after erasing the phonon background the remaining structure is used as new initial condition at $t = 20$. Left panel: evolution of particles velocity distribution for the time interval $t = 0$–50; right panel: particles velocity distribution at $t = 50$.

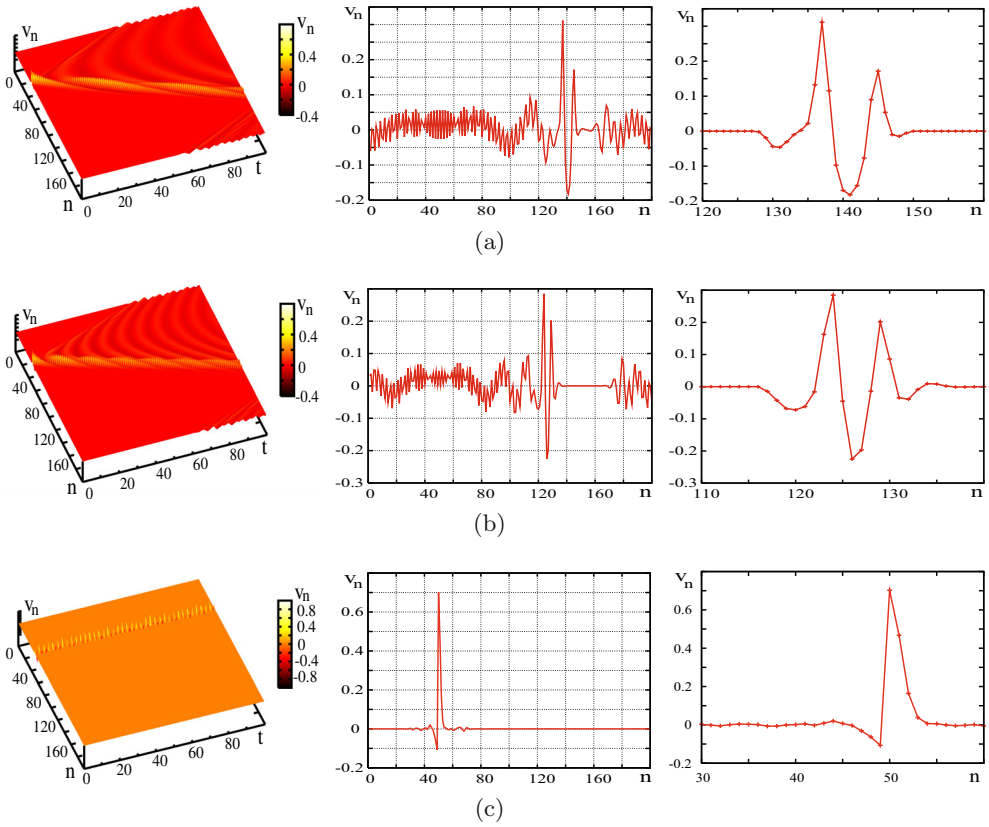

Fig. 8. Morse-Morse chain ($N = 200$). Localized excitations as the result of an initial kick to a single unit at constant $\eta_D = 0.4$ for different values of $\eta_b = 0.5$ (a), 1.0 (b) and 8.0 (c). Each horizontal panel, left to right, illustrates the time evolution of the velocity distribution $v_n(t)$ after 100 time units. The center pictures display the snapshot at $t = 100$ and the extreme right pictures provide a straightforward zooming of a few dozen sites lattice interval in order to see the internal structure of the localized excitation.

as a two-peak moving structure with alternating amplitudes of peaks. In other words, it may be considered formally as a modulated pulse (a mobile DB/ILM) in which the modulating envelope proceeds to the right with velocity $v_{\rm loc}$ while the modulated periodic wave moves to the left. The pulse is quite narrow, only two-three times wider than the period of the "carrier wave". The time period of the carrier $T_{\rm period}$ decreases with increasing relative influence of on-site force (parameters η_b and η_D) accompanied by falling velocity $v_{\rm loc}$. Eventually the moving structure becomes immobile as a pinned narrow one-peak DB/ILM (Fig. 8c). We have also observed the transformation from a multi-peak structure to a one-peak structure in our numerical simulations for $\eta_b \approx 4$ with $\eta_D = 0.4$ (not shown in Fig. 8). Such case gives the transformation in the dependence of the velocity $v_{\rm loc}$ (Fig. 10a) and of the value of $2\pi/T_{\rm period}$ (Fig. 10b) as functions of the parameter η_b for $\eta_D = 0.4$ (that is corresponding to the case presented

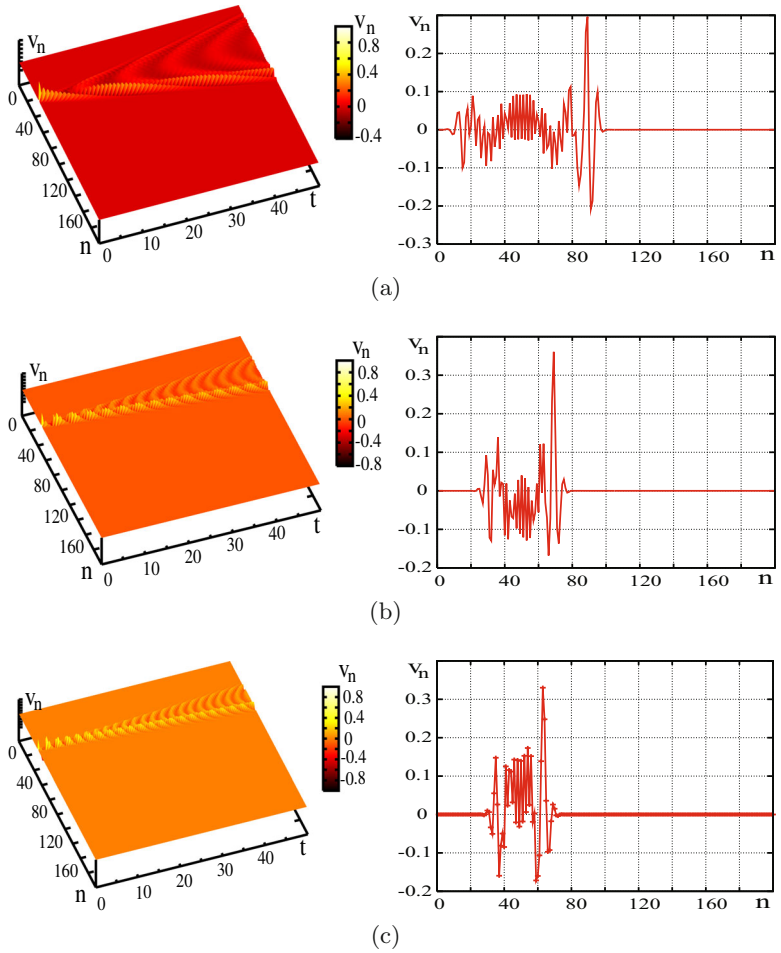

Fig. 9. Morse-Morse chain ($N = 200$). Localized excitations as the result of an initial kick to a single unit at constant $\eta_b = 2$ for different values of $\eta_D = 0.1$ (a), 1 (b) and 2 (c). Each horizontal panel, left to right, illustrates the time evolution of the velocity distribution $v_n(t)$ for 50 time units with cross-sections at $t = 50$.

in Fig. 8). The velocity falls very fast with increasing η_b reaching a very small value at $\eta_b \approx 4$. Apparently the ultimate localized structure may be classified as a mobile DB/ILM for $\eta_b < 4$ and as a pinned one for $\eta_b > 4$ for the chosen value $\eta_D = 0.4$. Such mobile-pinned transformation feature depends indeed on the value assigned to the parameter η_D whose influence is much more dramatic than that of parameter η_b as Figure 9 illustrates for $\eta_b = 2$ and different values of η_D.

5 Role of transverse motions: solitons, DB/ILM and more

As earlier emphasized in a "transversal" lattice (Fig. 2b) if the on-site bond is symmetric, or in our case weak enough hence harmonic, a strong initial pulse of velocity excites simultaneously the two identical localized modes, symmetrically moving away from the point of excitations in opposite directions. Choosing $v_0 = 1$ as in the case considered above for a "longitudinal" chain with no on-site potential (Figs. 6 and 7) one may indeed observe the two solitons as illustrated in Figure 11, moving right-to-left and left-to-right, respectively, with velocity slightly above the sound velocity but smaller than the corresponding value in the solely "longitudinal" chain. It is because in the "transversal" lattice the energy of each excited soliton is twice less than that in the longitudinal lattice for the same level of excitation. The other feature is the peculiar distribution of coordinates of particles between solitons (Fig. 11, right panel) – if particles deviate from equilibrium positions the same distance there is no restoring force (at least, it is small for small difference of positions of neighboring particles) and particles may keep their position far from the initial location for quite long time. In other words, we have two connected kinks. Noteworthy is that in the theory of DNA-like wires [11,24], structures with transverse shifts of particles, such space distributions of sites are called "bubbles". But if there is an on-site force, however weak, bubbles resolve fast but the solitonic structure changes little though the velocity of localized excitations decreases and may become slightly subsonic. In view of the above such mobile breathers associated with a bubble may be denoted as bubble-breathers [24]. It should also be added

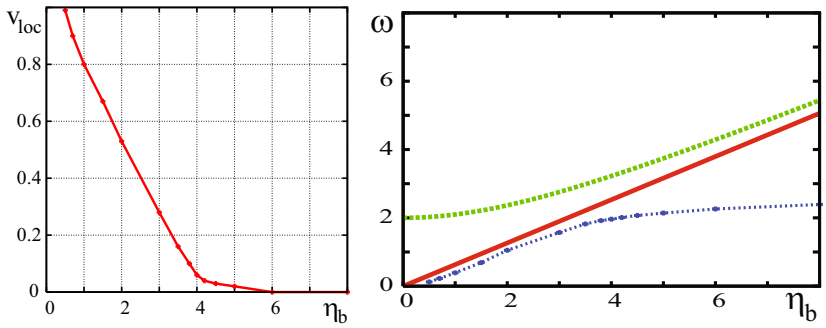

Fig. 10. Morse-Morse lattice: role of parameters describing the relative influence of on-site to inter-site potentials. Left panel: velocity $v_{\rm loc}$ and right panel: frequency $\omega = 2\pi/T_{\rm period}$ vs. η_b at constant $\eta_D = 0.4$. The curves in the right panel correspond to ω_{cr1} (blue, bottom line), ω_{cr2} (green, upper line) (with the phonon band in-between them) and $\omega = 2\pi/T_{\rm period}$ (red, middle line). It appears that ω_{cr1} and ω_{cr2} grow with increasing η_b while the phonon band shrinks; the value $\omega = 2\pi/T_{\rm period}$ (considered as breather frequency in some sense) grows too keeping its value only slightly less than ω_{cr1} for $\eta_b < 4$ and dramatically falls below ω_{cr1} with $\eta_b < 4$.

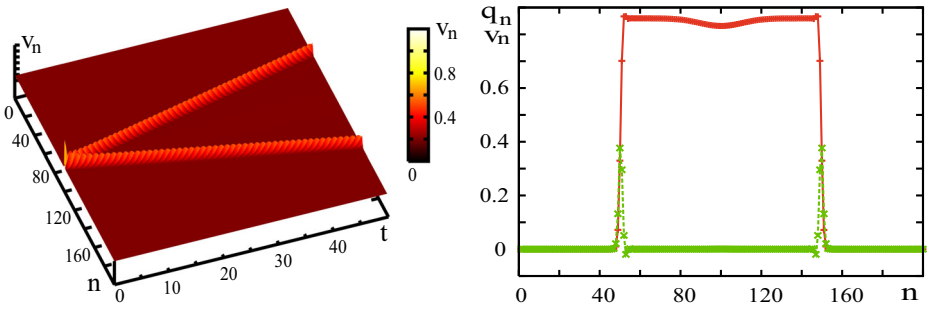

Fig. 11. Morse-Morse "transversal" lattice ($N = 200$) with transverse deviations of its units albeit without on-site potential ($\eta_b = \eta_D = 0$). Two highly-energetic identical solitons, symmetrically oppositely moving, are excited following an initial kick to the particle $n = 100$ with $v_0 = 1$. Left panel: evolution of particles velocity distribution for time interval $t = 0$–50; right panel: snapshot of particles velocity v_n (green, line of crosses) and deviation q_n (red, dotted line) distributions at $t = 50$. The soliton velocity is slightly above the sound velocity.

that a chain without on-site bonds is again one of two asymptotic models, in contrast to the case with a dominant on-site potential, which is the case of the PB model of DNA [11,23,24]. In most works using the PB model the parabolic potential well of inter-site interactions is generally taken very large relative to the corresponding features of the on-site potential well. Here, however, such situation is the case only when the parameter η_D is large enough and the parameter η_b is small enough. Then with increasing stiffness of the on-site potential solitons transform to mobile breathers (Fig. 12b) and then to pinned breathers (Fig. 12c). Overall this occurs very much like in the longitudinal case. Finally, in a "transversal" lattice the domain occupied by phonons, which accompany the localized modes created following the initial pulse, is concentrated between soliton-like excitations where the phonons form a standing wave. Further details on this matter can be found in reference [24].

6 Conclusion

The transformation of (supersonic) solitons to pinned breather-like (DB/ILM) excitations via a stage of mobile localized structures has been studied in anharmonic lattices of particles interacting with inter-site and on-site Morse forces. First we have considered solely unidirectional longitudinal motions, hence only along the one-dimensional geometrical structure of the lattice. The study has permitted to illustrate the influence of the ratio of on-site to inter-site potential strengths. For simplicity the case of excitations of localized modes by a strong initial pulse externally applied to a single lattice unit has been studied. It has been shown that supersonic solitons, excited in the lattice without on-site dynamics, transform first to mobile breather-like modes as the on-site potential is turned on and grows in relative strength. The DB/ILM velocity decreases with the increasing influence of the on-site potential and pinned breathers are the ultimately surviving excitations if the on-site potential largely overwhelms the inter-site one. In a second approach to the Morse-Morse competing dynamics we have also considered two-dimensional-like Morse-Morse lattices with transverse motions of particles along the (longitudinal) line but away from it, hence moving orthogonal to the lattice backbone structure. In such a case two symmetric identical localized modes moving in opposite directions, a soliton-like and a mobile breather-like, are excited by short localized initial

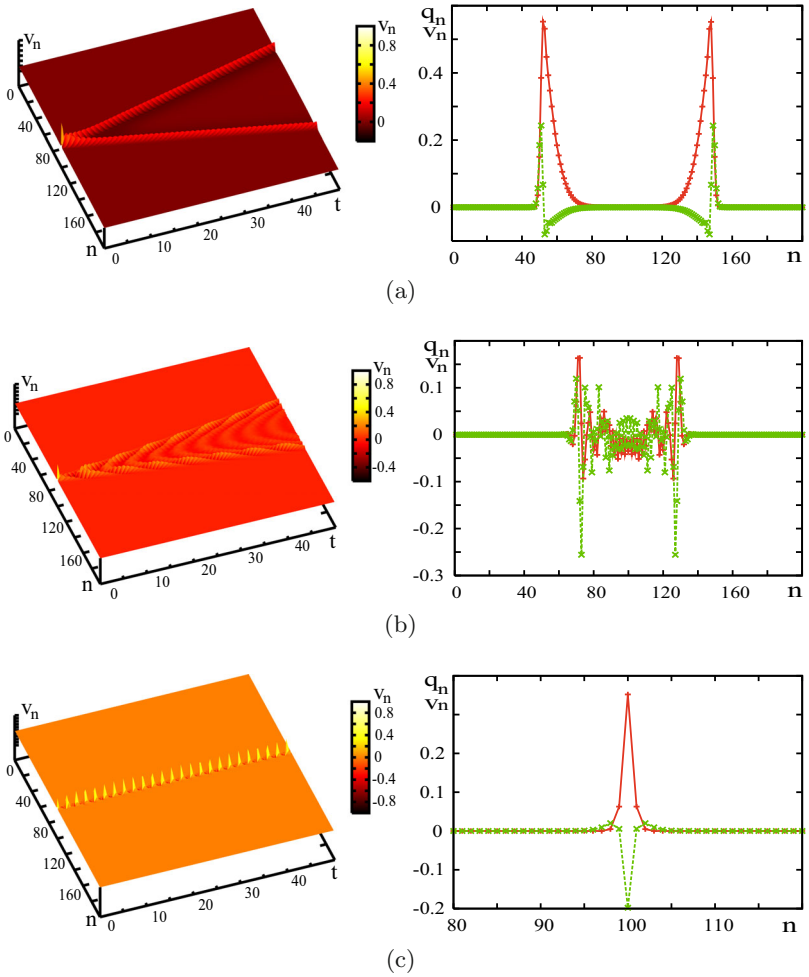

Fig. 12. Morse-Morse "transversal" lattice ($N = 200$). Evolution of excitations due to the initial kick to a single particle at constant $\eta_D = 0.4$ and different values of η_b. On each horizontal panel, left to right, it is shown the time evolution of velocity distribution $v_n(t)$ for 50 time units with snapshots v_n (green, lines of crosses) and q_n (red, dotted lines) at $t = 50$ for (a) $\eta_b = 0.5$, (b) 2.0 and (c) 6.0.

pulses in the lattice if the inter-site potential is strong enough. Formation of bubbles (in the language of DNA-like molecular wires [11,23,24]), bubble-breathers and pinning breathers are observed if the on-site bond overwhelms the inter-site interaction.

Author contribution statement

All authors contributed equally to the paper.

A.P.C., W.E. and M.G.V. are grateful to Prof. E. Schöll for his hospitaly at the Institut für Physik, Technische Universität Berlin, in the framework of the Collaborative Research Center 910: "Control of self-organizing nonlinear systems: Theoretical methods and concepts of application" (Sonderforschungsbereich 910) funded by Deutsche Forschungsgemeinschaft. The authors also acknowledge Prof. J.F.R. Archilla for correspondence and enlightening suggestions. A.P.C. and V.D.L. acknowledge support under Project 16-11-10163 and S.V.D. acknowledges support under Project 16-12-10175, both projects from the Russian Science Foundation.

References

1. A.A. Ovchinnikov, Sov. Phys. J. Exp. Theor. Phys. **30**, 147 (1970)
2. A.A. Ovchinnikov, S. Flach, Phys. Rev. Lett. **83**, 248 (1999)
3. A.M. Kosevich, A.S. Kovalev, Sov. Phys. J. Exp. Theor. Phys. **40**, 891 (1975)
4. A.S. Dolgov, Sov. Phys. Solid State **28**, 907 (1986)
5. A.J. Sievers, S. Takeno, Phys. Rev. Lett. **61**, 970 (1988)
6. J.B. Page, Phys. Rev. **41**, 7835 (1990)
7. S.A. Kiselev, S.R. Bickham, A.J. Sievers, Phys. Rev. B **48**, 13508 (1993)
8. D.K. Campbell, S. Flach, Yu.S. Kivshar, Phys. Today **57**, 43 (2004), and references therein
9. S. Flach, A.V. Gorbach, Phys. Rep. **295**, 181 (2008), and references therein

10. S.V. Dmitriev, E.A. Korznikova, Yu.A. Baimova, M.G. Velarde, Phys. Usp. **59**, 446 (2016), and references therein
11. T. Dauxois, M. Peyrard, *Physics of Solitons* (Cambridge University Press, Cambridge, 2006)
12. N.J. Zabusky, M.D. Kruskal, Phys. Rev. Lett. **15**, 240 (1965)
13. N.J. Zabusky, Comput. Phys. Commun. **5**, 1 (1973)
14. M. Toda, *Theory of Nonlinear Lattices*, 2nd edn. (Springer, Berlin, 1989)
15. V.I. Nekorkin, M.G. Velarde, *Synergetic Phenomena in Active, Lattices. Patterns, Waves, Solitons, Chaos* (Springer, Berlin, 2002)
16. P.W. Anderson, Phys. Rev. **109**, 1492 (1958)
17. A. Ranciaro Neto, M.O. Sales, F.A.B.F. de Moura, Solid State Commun. **229**, 22 (2016)
18. S. Aubry, Physica D **103**, 201 (1997)
19. S. Aubry, Physica D **216**, 1 (2006)
20. G. Iooss, G. James, Chaos **515**, 015113 (2005), and references therein
21. D. Hennig, C. Mulhern, L. Schimansky-Gaier, G.P. Tsironis, P. Hänggi, Phys. Rep. **586**, 1 (2015)
22. L. Cisneros-Ake, L. Cruzeiro, M.G. Velarde, Physica D **306**, 82 (2015), and references therein
23. M. Peyrard, A.R. Bishop, Phys. Rev. Lett. **62**, 2755 (1989)
24. A.P. Chetverikov, W. Ebeling, V.D. Lakhno, A.S. Shigaev, M.G. Velarde, Eur. Phys. J. B **89**, 101 (2016), and references therein
25. J. Dancz, S.A. Rice, J. Chem. Phys. **67**, 1418 (1977)
26. T.J. Rolfe, S.A. Rice, J. Dancz, J. Chem. Phys. **70**, 26 (1979)
27. A.P. Chetverikov, W. Ebeling, M.G. Velarde, Int. J. Bifurc. Chaos **16**, 1613 (2006)